

MULTI-LEVEL MODULATION IN THE INDOORS LEAKY FEEDER ENVIRONMENT

J. M. Torrance, T. Keller and L. Hanzo

Dept. of Electr. and Comp. Sc., Univ. of Southampton, SO17 1BJ, UK.

Tel: +44 17 03 59 31 25, Fax: +44 17 03 59 30 45

Email: jmt94r@ecs.soton.ac.uk, tk@ecs.soton.ac.uk and lh@ecs.soton.ac.uk

http://rice@ecs.soton.ac.uk

ABSTRACT

Leaky feeders offer the prospect of high average Signal to Noise Ratio (SNR) in an indoors environment. The signal is transmitted from a series of slots acting as antennae and superposition of the paths results in fades of up to 25 dB below the mean signal level. A model is presented for the propagation path between the leaky feeder Base Station (BS) antenna and a single omni-directional receiver antenna, which was verified using measurements. The Bit Error Rate (BER) performance of such a system is investigated for 1, 2 and 4 bits per symbol, coherent and non-coherent modulation schemes. These are compared with the performance of a more conventional indoor BS antenna.

1. INTRODUCTION

This paper presents a model simulating the propagation path between a leaky feeder transmitter and a single omni-directional receiver antenna in an indoors environment. The model is verified by comparing simulated and measured impulse responses. The model is then used to simulate the up and down links for one user in a DECT (Digital European Cordless Telephone) system. This is compared with the performance of a single omni-directional to another single omni-directional antenna, in the same environment. The BER performance of 1, 2 and 4 bits per symbol coherent and noncoherent modulation schemes are then presented for both antenna arrangements.

2. LEAKY FEEDER

2.1. Propagation model

Leaky feeders are a type of distributed antennae. They were originally conceived to provide subterranean radio propagation in train tunnels and coal mines. They have recently been considered as an alternative to conventional antennae for indoors micro-cells [1]. They are constructed from coaxial cable where the outer shield is perforated with a series of holes. The coaxial cable is typically about one hundred metres long and can be threaded through a building offering radio illumination in a way that would require many individual omni-directional antennae. Fabrication costs are relatively cheap and deployed intelligently, leaky feeders can reduce network infrastructure costs. The propagation model presented considers the path between a leaky feeder and a

single omni-directional antenna without taking account of the detailed geometry of the building upon the radiation from each slot of the leaky feeder. The model is restricted to two dimensions, only the relative signal strength is considered and reciprocity is assumed. The leaky feeder¹ used was constructed of a 0.5" diameter copper foil outer and a foam polyethylene dielectric inner. It had transverse slots pseudo-randomly distributed with a minimum and maximum spacing of 0.01 m and 0.3 m, respectively. The feeder's linear axial attenuation κ was 0.15dB/m at a frequency of 2 GHz, the relative phase velocity β was 0.88. The model uses a ray-tracing technique in conjunction with Devasirvatham's [2] model for indoors path loss. Each transverse leaky feeder slot is approximated by the radiation profile of a dipole antenna. The leaky feeder was modelled as a group of radiating dipoles lying on the $y = 0$ axis of a two dimensional plane, with the input at $x = 0$ and N slots at coordinates $(D(n), 0)$ for $n = 1, 2, \dots, N$. Let $P = Ae^{j\phi}$, an idealised impulse of amplitude A and phase ϕ , propagate along the leaky feeder from $x = 0$ at a velocity of $c \cdot \beta \text{ ms}^{-1}$, where c is the speed of light in free space. The impulse will take $t_1(n) = D(n)/(\beta c)$ seconds to travel to slot n . The attenuated and phase-rotated impulse at this point is described in (1), where λ is the free space wavelength:

$$S(n) = 10^{-\frac{D(n)\kappa}{20}} Ae^{j(\phi + (\frac{2\pi\beta D(n)}{\lambda}))}. \quad (1)$$

The propagation distance from the n^{th} slot to a receiver at (R_x, R_y) is given by (2) for $n = 1, 2, \dots, N$:

$$R(n) = \sqrt{(R_x - D(n))^2 + R_y^2}. \quad (2)$$

A free space propagation velocity is assumed once the impulse has left the cable and hence the impulse takes $t_2(n) = R(n)/c$ seconds to travel from the n^{th} slot to (R_x, R_y) .

By treating each slot as an independent dipole, it can be assumed that the radiation pattern of each slot relates the transmitted power in a given direction, to the cosine of the angle, θ , between the direction of propagation and a perpendicular to the cable. It can be seen that the received impulse at the antenna is given by (3), where $M(R(n))$ is the amplitude path loss from slot n to the receiver antenna

¹The authors would like to express their gratitude to Professor Raymond Steele for initiating the project, to Mr David Stewart and Terry Mitchell for their help during its execution and to Mr. Davies at RFS Hanover for the supply of the Leaky-Feeder cable.

at position (R_x, R_y) .

$$Q(n) = S(n) \cdot \cos(\theta) \cdot M(R(n)) \cdot e^{j \frac{R(n)}{c\lambda}} \quad (3)$$

Devasirvatham's model is used in the following form:

$$M(r) = \left[r \cdot 10^{\left(\frac{0.7 \cdot r}{20} + 1.925 \right)} \right]^{-1} \quad (4)$$

Using a similar technique to [3] for calculating the sum of an ensemble of paths and letting t represent time, it can be seen that the impulse response is given by:

$$h(t) = \begin{cases} Q(n) & \text{if } t = t_1(n) + t_2(n) \\ 0 & \text{otherwise.} \end{cases} \quad (5)$$

A series of impulse response measurements were made from a leaky feeder to an omni-directional antenna, using a Swept Time Delay Cross Correlator (STDCC). Impulse responses calculated using (5) are of a much higher resolution than the measured results and must be post processed in order to enable a reasonable comparison. Since the average auto-correlation $\psi'(n)$ of the STDCC pseudo-noise sequence is not an ideal impulse-like autocorrelation function, it follows from [4] that the STDCC's estimated output signal is given by:

$$y(t) = \sum_{k=-\infty}^{+\infty} h(k) \cdot \psi'(t-k). \quad (6)$$

The average auto-correlation is used because in practice the STDCC receiver will not be perfectly aligned with the transmitter and this will result in the receiver's sampling points not always falling on the auto-correlation peaks. The STDCC receiver partly avoids this problem by taking the average of every two measurements. The post processing must take this into account. From [5] we can arrive at (7), which is an expression for the auto-correlation of the PN sequence $\psi(k)$:

$$\psi(k) = \begin{cases} m - (m+1) \cdot k & \text{if } |k| \leq 1 \\ -1 & \text{otherwise,} \end{cases} \quad (7)$$

hence we have:

$$\psi'(k) = \frac{\psi(k) + \psi(k+1)}{2} \quad (8)$$

Finally, as the STDCC only has a resolution of $20ns$, the simulated impulse response is averaged into $20ns$ bins, which allows the generation of a comparable number of sample points for both the simulated and measured results.

Figure 1 shows a measured impulse response and simulated impulse responses using the free space path loss, and Devasirvatham's model after post-processing. The Figure portrays a comparison at (R_x, R_y) equal to $(15,3)$ m. The free space model predicts an impulse response with a higher delay spread than that measured, while Devasirvatham's model follows the measured result more closely. Further comparisons between the measured and modelled scenarios showed that when the receiver was very close (less than 1 metre) to the cable the models were less accurate.

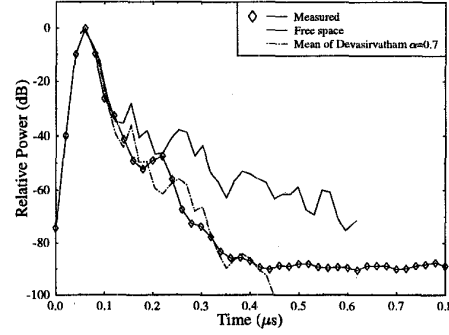


Figure 1: Measured and simulated impulse responses between a leaky feeder positioned along the $y = 0$ and a single omni-directional antenna positioned at $(15,3)$

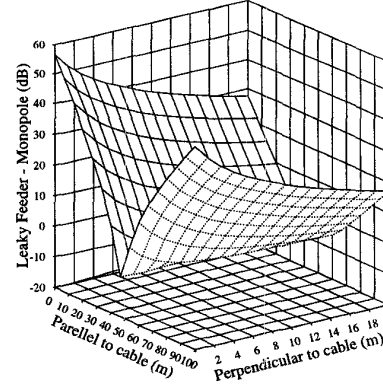


Figure 2: Three dimensional plot of the received signal level difference between an omni-directional antenna positioned at $(50,0)$ and a 100 m leaky feeder positioned along the $y = 0$ axis

2.2. Pathloss

In this Section we contrasted the pathloss of the leaky feeder with that of a conventional omni-directional antenna by plotting the difference between their received signal levels as a function of the receiver's position, while using an identical transmitted power. The three-dimensional plot of Figure 2 shows that the leaky feeder has a higher average received signal level than a single omni-directional antenna and it can offer up to 50 dB reduction in propagation loss compared with the single omni-directional antenna. By contrast, the single omni-directional antenna never offers more than 10 dB benefit, which is limited to the narrow valley in the centre of the Figure. Figure 3 shows more clearly that the leaky feeder gives an improved SNR for over 75% of the floor space compared with a single omni-directional antenna.

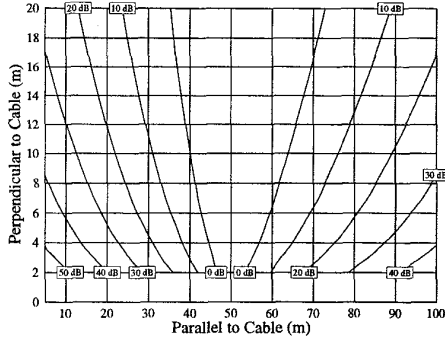


Figure 3: Contour plot of the received signal level difference between an omni-directional antenna positioned at (50,0) and a 100 m leaky feeder positioned along the $y = 0$ axis. The area between the 0 dB contour-lines represents the region where the omni-directional antenna's path loss is lower

2.3. Delay Spread

The root mean squared (RMS) delay spread, Δ , is defined as

$$\Delta = \left[\frac{\int_{-\infty}^{\infty} (t - D)^2 \cdot h(t) dt}{\int_{-\infty}^{\infty} h(t) \cdot dt} \right]^{\frac{1}{2}} \quad (9)$$

where D is the mean delay. The mean delay, D , and the RMS delay spread, Δ , can be calculated for the simulated impulse response given in (5). Figures 4 and 5 show these values for $-10 \text{ m} < x < 110 \text{ m}$ and $0 \text{ m} < y < 20 \text{ m}$. From Figure 4 it is apparent that the largest contribution to the mean delay of the signal, results from the relative phase velocity of the leaky feeder, β . This is because the gradient along the parallel axis, for $0 \text{ m} < x < 100 \text{ m}$, is much greater than that along the perpendicular axis or other points along the parallel axis. The minimum delay is at the point closest to the input of the leaky feeder, however, even the maximum delay, $0.5 \mu\text{s}$ is much less than the guard band in DECT TDMA frames of $60 \times 868 \text{ ps} = 52 \mu\text{s}$. Figure 5 illustrates the delay spread, which is the most relevant statistical parameter in determining the maximum symbol rate that can be sustained by the channel without encountering significant dispersion. There is a trend towards increased delay spread with an increase in the Y coordinate. This is particularly true in the central region of the cable where the greatest number of sources make the largest contribution to the received signal. At either end of the cable the delay increases, particularly at $X < 0$. The problems caused by this can be minimised by ensuring the cable runs from wall to wall with the building.

2.4. Simulation of a DECT channel

DECT has a symbol rate of 1152 kBd using TDD/TDMA where there are 12 up link followed by 12 down link time slots, every 10 ms. Each slot contains 420 data symbols and 30 leading and 30 trailing guard band symbols. The floor of a building of length x and width y where $0 \text{ m} < x < 100 \text{ m}$

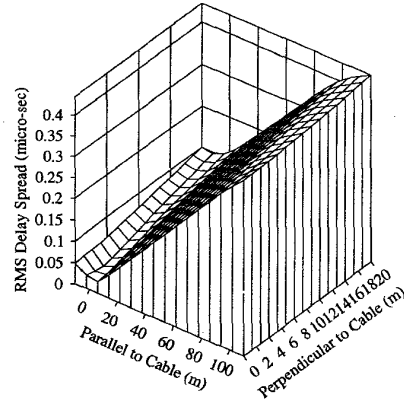


Figure 4: Mean delay in the region $-10 \text{ m} < x < 110 \text{ m}$ and $0 \text{ m} < y < 20 \text{ m}$ with a leaky feeder positioned along the $y = 0$ axis

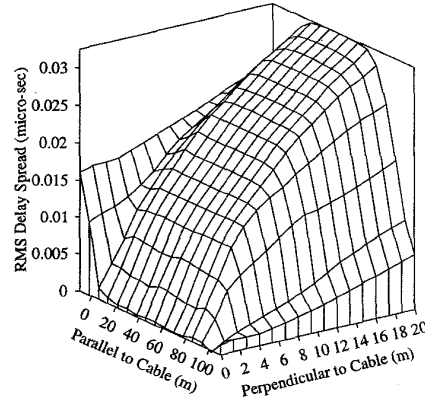


Figure 5: RMS delay spread in the region $-10 \text{ m} < x < 110 \text{ m}$ and $0 \text{ m} < y < 20 \text{ m}$ with a leaky feeder positioned along the $y = 0$ axis

and $-20 \text{ m} < y < 20 \text{ m}$ was considered. The leaky feeder was placed along the $y = 0$ axis and symmetry of propagation was assumed along this axis. A duplex channel was simulated between the leaky feeder and a portable station (PS) equipped with an omni-directional antenna moving at 0.5 ms^{-1} along the $y = 10$ axis. This was achieved by performing vectorial addition of the signal components received at the omni-directional antenna from each of the leaky feeder slots. Therefore the received signal $T(R_x, R_y)$ is given by:

$$T(R_x, R_y) = \sum_{n=1}^N Q(n). \quad (10)$$

This addition was performed for each transmitted or received symbol.

2.5. Fading Characterisation

The fading profile between the leaky feeder and the single antenna can be seen in Figure 6. Each marker in this Figure

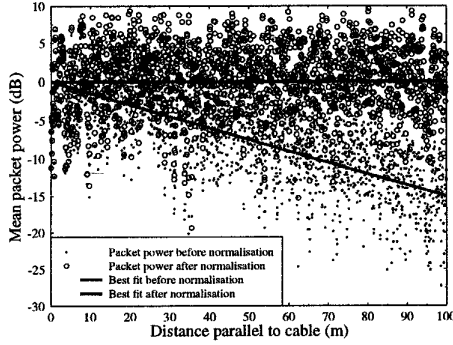


Figure 6: Mean path loss before and after power normalisation of 15 dBm^{-1} calculated in blocks of 100 ms for the up and down slots of the first user in a DECT system along the $y = 10$ axis with a leaky feeder along the $y = 0$ axis, mobile velocity of 0.5 ms^{-1}

represents the average power of the symbols that constitute 10 up link and 10 down link slots. The 15 dBm^{-1} linear attenuation of the leaky feeder is explicit in the Figure, but in order to consider probability density function (PDF) the fading, this factor is removed from the fading by normalising. The effect of normalisation is also seen in Figure 6.

Having removed the 15 dBm^{-1} linear attenuation factor from the channel, a histogram of the fade depths can be generated. In preference to calculating a single histogram for the whole channel, 1 m (or 2s) segments were considered and plotted in Figure 7. From this it is clear that the PDF of fade depths is similar over the distance range of $0 \text{ m} < x < 100 \text{ m}$. In the multipath environment of the randomly distributed slots there is no dominant line-of-sight (LOS) path, hence simple logic would dictate that the fading is Rayleigh. However, comparison of the experimental PDFs with a Rayleigh distribution reveals that the fades are less deep, since the fade depth is reduced by the mildly dispersive channel.

3. MODEM PERFORMANCE

In our further investigations the BER performance of coherently and noncoherently detected 1, 2 and 4 bits per symbol modems was studied in the indoors environment of the leaky feeder, assuming a DECT-like TDD system signalling at 1152 kbaud irrespective of the number of modulation levels. Since the symbol interval length is nearly $1 \mu\text{s}$, the $0.03 \mu\text{s}$ dispersion seen in Figure 5 allows us to consider the channel to be essentially non-dispersive and derive BER results using the leaky feeder fading envelope of Figure 6. These will be contrasted with the BERs of the conventional omni-directional antennae. For noncoherent modulation there were 421 symbols per frame, the first symbol being the reference for demodulation of the first data symbol, while for coherent modulation there were 422 symbols per frames with a pilot symbol both at the start and end of the data block. The pilot symbols were used to estimate and hence compensate for channel fading. Perfect

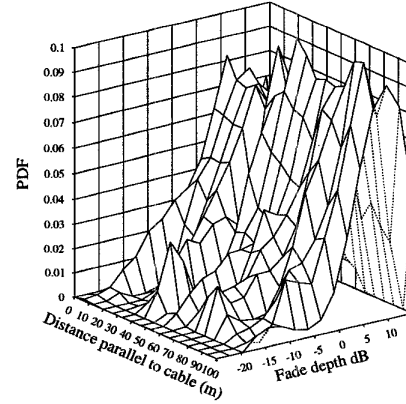


Figure 7: Segmented PDF of fading profile taken every 1m, along the $y = 10$ axis with a leaky feeder along the $y = 0$ axis, mobile velocity of 0.5 ms^{-1} , considering the up and down slots of the first user in a DECT system. All measurements were made after normalising for the linear attenuation factor

clock and carrier recovery were assumed.

The simulated BER experiments were conducted for the leaky feeder channel as described in Section 2.4. The fading PDF is similar along the length of the leaky feeder, as shown in Figure 7. Removing the 15 dB bias from the simulated leaky channel before performing the BER experiments, permits the generation of SNR versus BER curves that are independent of the position of the omni-directional receiver antenna relative to the leaky feeder. In reference [7] we have shown that for reasonable velocities the performance of linearly interpolated pilot symbol assisted modems (PSAM) will not deteriorate significantly with respect to more complex interpolators. Therefore, given that the channel can be assumed to behave in a narrowband fashion, the BER performance of the various modulation schemes is only dependent upon the mean SNR.

The BER performance of the modulation schemes was evaluated for both the leaky feeder channel model and for a conventional omni-directional scenario using the best-case Gaussian channel and the worst-case Rayleigh channel. The Rayleigh channel had a normalised Doppler frequency equivalent to that of the leaky feeder channel. The BER performance over the leaky feeder channel is expected to be between the upper and lower bound of the conventional omni-directional antenna.

Figure 8 shows the performance of all the modulation schemes through the leaky feeder channel. The usual acronyms are used, namely Binary Phase Shift Keying (BPSK) and its differential version DBPSK, Quaternary Phase Shift Keying (QPSK) and DQPSK as well as Quadrature Amplitude Modulation [7] with a coherent maximum minimum distance square (SQ) constellation and the non-coherent star (ST) constellation. As expected, the coherent schemes perform better than the equivalent differential, noncoherent schemes, where the difference is greater with more modulation levels. Figures 9 and 10 show the performance in Rayleigh and Gaussian channels for the corresponding omni-directional schemes. As expected, the leaky feeder BER

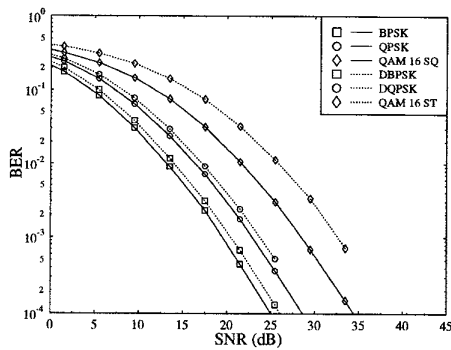


Figure 8: BER for a mobile travelling at 0.5ms^{-1} along the $y = 10$ axis with a leaky feeder along the $y = 0$ axis. Results are the average BERs for up and down-link slots of the first user in a DECT system. Differential modulation deploys a single pilot at the beginning of a DECT frame and coherent modulation deploys PSAM and a pilot at the beginning and end of the frame.

curves are between that of a Gaussian channel and a Rayleigh channel.

16QAM performs between 7 and 15 dB better over the conventional Gaussian scenario than in the leaky feeder channel. In order to compensate for the performance degradation induced by the inherent multipath characteristics of the leaky feeder, the SNR benefit of the leaky feeder must exceed these values in stationary situations. From Figure 3 it can be observed that the leaky feeder does offer more than 15 dB improved SNR over most of the illuminated floor space. In the more typical case of non-LOS Rayleigh channels the benefit of the leaky feeder will be even more prevalent. A range of further interesting conclusions can be gleaned from the detailed examination of Figures 8-10.

4. CONCLUSIONS

A simulation model of the leaky feeder channel has been presented and verified by impulse response measurements. The BER performance of the channel between a mobile receiver and the leaky feeder has been considered for various modulation schemes. The leaky feeder typically offers higher average SNR than a single omni-directional antenna, which is associated with inherent multi-path propagation.

5. REFERENCES

- [1] Kevin J. Bye, "Leaky-feeders for cordless communication in the office," in *IEEE Eurocon*, pp. 387-390, IEEE, 1988.
- [2] D. M. Devasirvatham, "Multi-frequency propagation measurements and models in a large metropolitan commercial building for personal communications," in *IEEE PIMRC*, pp. 98-103, IEEE, 1991.
- [3] K.W.Cheung, R.D. Murch and C.C. Ling, "The fading characteristics of distributed antennas for indoor

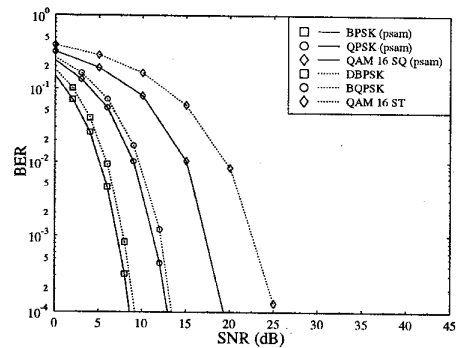


Figure 9: BER in Gaussian Channel with DECT frame structure

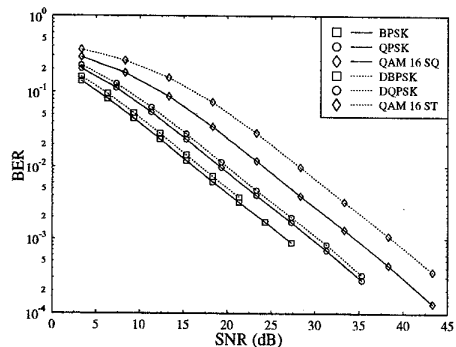


Figure 10: BER in Rayleigh Channel with normalised Doppler frequency equivalent to a mobile velocity of 0.5ms^{-1} in a DECT-like system

wireless systems," in *Fourth IEEE International Conference on Universal Personal Communications Record*, pp. 377-381, IEEE, 1995.

- [4] J. D. Balcomb, H. B. Demuth and E. P. Gyftopoulos, "Cross-correlation method for measuring the impulse response of reactor systems," *Nuclear Science and Engineering*, vol. 11, pp. 159-166, 1961.
- [5] J. D. Parsons, D. A. Demery, A. M. Turkmani, "Sounding techniques for wide-band mobile radio channels: A review," *IEE Proceedings-I*, vol. 138, no. 5, pp. 437-446, 1991.
- [6] W.T. Webb, L. Hanzo: *Modern quadrature amplitude modulation: Principles and applications for fixed and wireless channels*, IEEE Press-Pentech Press, 1994, ISBN 0-7273-1701-6, p 557
- [7] J. M. Torrance and L. Hanzo, "Comparative study of pilot symbol assisted modem schemes," in *IEE Conference on Radio Receivers and Associated Systems*, pp. 36-41, IEE, 1995.